Journal of Membrane Science & Research

journal homepage: www.msrjournal.com

Research Paper

The Experimental, Technical, and Economical Evaluations of Green Fabricated Activated Carbon/PVA Mixed Matrix Membrane for Enhanced CO_2/CH_4 Separation

Abolfazl Jomekian [1, *], Bahamin Bazooyar [2], Seyed Ali Akbar Mansoori [3]

[1] *Esfarayen University of Technology, Esfarayen, North Khorasan, Iran*
[2] *Centre for Climate and Environmental Protection, Cranfield University, Bedford, Bedfordshire, MK43 0AL, UK*
[3] *Engineering & Technical Services, Process Engineering Department, South Pars Gas Complex Company, Assaluyeh, Iran*

Article info

Received 2022-10-18
Revised 2022-12-26
Accepted 2023-01-13
Available online 2023-01-13

Keywords

Tea waste
Carbonated soft drink waste
Activated carbon
CO_2/CH_4 separation
Techno-economical evaluation

Highlights

- Raw carbon powders were synthesized from black tea and carbonated soft drink wastes
- The activated carbon powders were incorporated into the matrix of PVA
- Membrane lifetime and plant lifetime have huge effects on total costs of the system.

Graphical abstract

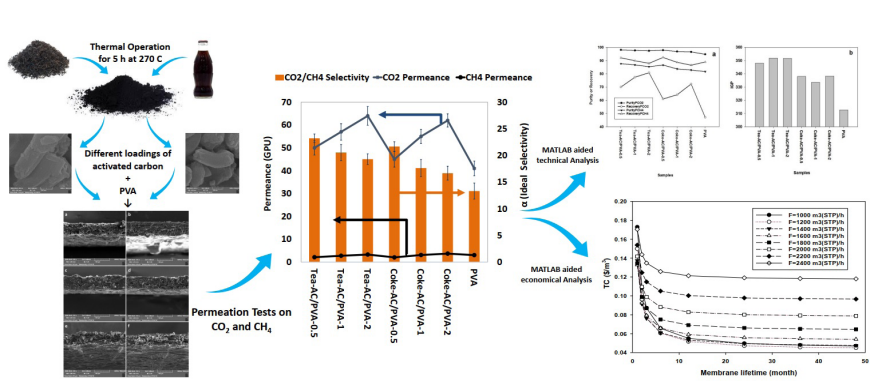

Abstract

In the experimental part of the work, carbon powders were synthesized and then activated in this work from tea and carbonated soft drink (coke) wastes. The synthesized activated carbon (AC) particles were incorporated into the matrix of PVA to form mixed matrix membranes (MMMs) to be examined for the separation of CO_2 from CH_4. SEM, FTIR, N_2 adsorption-desorption, DFT pore size distribution (PSD), and BET analysis were used for the characterization of MMMs. The applied permeation tests indicated that tea wastes were better precursors for the synthesis of ACs than coke for the removal of carbon dioxide from methane by AC/PVA MMMs. In the technical and economical evaluation of the work, MATLAB programming was used. The result of the techno-economical evaluation of membranes in a designed two-stage membrane separation configuration showed the maximum process global performance index (IGP) of 351.9 for a sample and it appeared that the CO_2 recovery was the most effective factor in IGP determination. The turbine for generating power was determined to be only economically interesting in the process with the lowest gas flow rates. The membrane lifetime and the plant lifetime were determined to be two of the most important parameters affecting the total costs of the system. Membranes with an average lifetime below 6 months and the plant lifetime below 20 years, cause a considerable rise in total costs of the system and potential economical failure of the designed system configuration.

1. Introduction

The production rate of food waste has increased dramatically in the recent decade worldwide mostly due to the rapid growth of population in cities and the alteration of people's lifestyles. These food wastes are mostly generated from domestic parts of cities. A staggering number of above 1.3×10^9 tons per day of food waste is happening now [1]. Food waste is occurring in all different stages of the food supply chain depending on the level of development of the country, the food industry infrastructure, and the consumption culture of the people. In general in developing countries, most of the food waste happens in the early stages of the food supply chain while in developed countries the consumers waste the main part of the supplied food in a huge amount nearly

* Corresponding author: abolfazl.jomekian@gmail.com, a.jomekian@esfarayen.ac.ir (A. Jomekian)

DOI: 10.22079/JMSR.2023.563685.1571

equal to the whole yearly food produced in some African countries [2]. In Iran, food is wasted from the early to late steps of the food supply chain on a huge scale [3]. If we neglect the wastes that happen in agricultural processes, the amount of food waste by consumers alone is also tremendous. According to Iran's Food Producers Cooperatives report, of 130 million tons of food produced per year for consumers, more than 19% is wasted meaning about 25 million tons [1]. Based on another report [4], the amount of wasted food in Iran by the consumer is more than enough to fight malnutrition across the whole country.

Among the food waste in Iran, black tea and carbonated soft drinks are considered to be two of the most consumed and wasted drinkable food materials. Iran has about 1% of the world's population, however, the Iranians consume over 5% of the world's produced black tea [5]. Therefore the number of tea waste must be huge considering the mentioned percentages. The per capita consumption of carbonated soft drinks in Iran is 42 liters per year which are beyond the global average. This means a huge amount of waste results from excessive consumption of carbonated soft drinks. This tremendous amount of generated food waste motivated the researchers to look for a variety of waste-managing methods and plans such as landfilling [6], composting [7], anaerobic digestion [8], fuel production from wastes [9], and thermal processes [10]. One of the most promising methods of food waste management is to convert these wastes to high-tech adsorbents such as activated carbons (AC)s by thermal methods [11]. This adsorbent can be synthesized from all three main types of food wastes [12, 13] and thermal processes such as combustion and pyrolysis have been used extensively for this purpose. ACs with high surface area and pore volume, applicable microporosity, and long life span are one of the most favorite carbon-based materials for the adsorption of hazardous vapors and gases such as CO_2, CO, H_2S, etc. [14, 15]. CO_2 is known to be the source of many industrial and environmental problems. Pipeline corrosion, hydrate formation in natural gas transmission, and global warming can be named as widely known ones. There are several different stablished methods for CO_2 capture, such as absorption by solvents, cryogenic operations, adsorption, chemical looping combustion, and membranes operations. The absorption by mostly amines suffers from considerable energy consumption and loss of solvent in adsorption-regeneration process and cause some environmental issues related to amine contamination, cryogenic operation consumes huge amount of energy which is not attractive in current world energy crisis, adsorption is an efficient method of CO_2 capture however this method is also energy demanding in process of changing temperature or pressure in TSA or PSA operations and capital cost of the operation may become remarkably high in high flowrates. Chemical looping combustion requires soling handling and dual reactors which are unattractive technically and economically. Hence, the capture of this gas by cost-effective and efficient methods is of great interest. Membrane processes are suggested as one of the most attractive methods of CO_2 separation. Investigations on the various inorganic, polymeric, and mixed matrix membranes (MMMs) for CO_2 separation have been developed to a large extent, especially in the last twenty years. Thin Film Composite (TFC) membranes, showed effectiveness in CO_2 separation [16, 17]. The selection of materials, design of configurations and modules, and determination of the concentration of solutions to fabricate selective layers are of utmost critical in the synthesis of mixed matrix membranes. Polyvinyl alcohol (PVA) is a cheap and widely accessible polymer with excellent film-forming ability, remarkable flexibility, high mechanical stability, and tensile strength. It has also confirmed resistance against hydrophobic materials but shows susceptibility toward water and moisture [18]. Remarkable works on the separation performance of this polymer blended with other polymers and inorganic or organic fillers have been reported in recent years. Barooah and Mandal [19] synthesized and examined the ZIF-8 /PVA/PEG mixed matrix membrane for CO_2/N_2 separation. They reported relatively high CO_2 permeance (86 GPU) with significantly enhanced CO_2/N_2 selectivity ($\alpha_{CO2/N2}$ =368). Torstensen et al. [20] reported the fabrication and performance investigation of PVA/nanocellulose MMMs for the separation of CO_2 from flue gas. In their work, the permeance of CO_2 and the CO_2/N_2 selectivity of synthesized MMMs showed increase from 105.5 to 127.8 GPU and from 36 to 39, respectively. The same material (PVA/nanocellulose) was tried by Jahan et al. [21] for the preparation of MMMs. They concluded that PVA/nanocellulose facilitated transport MMMs are notably superior to PVA regarding both permeance and selectivity. Guerrero et al.[22] prepared amino modified POSS/PVA MMMs for CO_2/N_2 separation. They reported that POSS could not satisfy the expectation for increase in CO_2 permeance due to the undesirable interaction of POSS with PVA, however PPO/PVA membrane in their work showed improvement of separation performance over PVA membrane.

Therefore, in the experimental part of this study as a new approach, two types of most common food waste in Iran were selected for the synthesis of ACs. Black tea wastes and carbonated soft drink wastes which are among the most observed and reported food wastes in Iran were selected as two different precursors for ACs synthesis. The resulting AC samples were separately introduced in the matrix of PVA with different loadings to yield AC/PVA MMMs. SEM, FTIR, N_2 adsorption-desorption analyses, BET surface area measurement, and DFT pore size profile analysis were utilized to characterize the prepared AC powder and prepared MMMs. The single-gas permeation examinations were conducted to evaluate the efficiency of synthesized membranes for the separation of CO_2 from CH_4.

As it is obvious the separation ability of the membranes is not understood if not evaluated in a simulated environment similar to industrially active system configurations. This could give us a proper perspective of the technical and economic viability of the proposed process and help us to decide to either scale up the process or leave it at the experimental level. There are numerous works on the technical and economical evaluation of the CO_2 separation in the previously published works using renowned commercial software such as Aspen Plus, Hysys, MATLAB, Microsoft Excel, etc., and some of them are provided in Table 1.

Table 1
Some previous works on the simulation of membrane separation processes using different software.

Simulation and/or Programming Software	Case Study	Ref.
Aspen$^+$ linked with Fortran	coal power plant flue gas, syngas in IGCC plant, and combustion	[23-26]
Aspen+ linked with MEMSIC	(natural gas) NG, gas in the furnace	[27-29]
Hysys linked with CAPCOST	furnace gas	[30-32]
Hysys linked with Visual Basic	NG	[33]
Hysys linked with Icarus	syngas	[34]
MATLAB	stack gas in power plant working by gas	[35,36]
MATLAB	stack gas in power plants working by coal	[37,38]
MATLAB	NG	[39,40]
Excel	syngas in the IGCC plant	[41]
Excel linked with Aspen$^+$	NG	[42]

In most of these works which includes one of our previously published works [42], the simulation is based on Aspen Plus programmed properties and equations and there is always a need for a link between a second programming language to modify the relationships and to link to Aspen Plus or Aspen Hysys through a user-defined subroutine. Moreover, there was always special attention to the energy requirement of the system and not to the possibility of generating energy from a designed membrane system configuration. Hence to fill the gaps found in previously published literature, we decided to use MATLAB programming to define the technical and economic relationships for sensitivity analysis of the CO_2/CH_4 separation process based on the data from a natural gas treatment plant.

2. Experimental

2.1. Materials

Black tea wastes (Ahmad®), and carbonated soft drinks (Coca-cola®) were supplied from domestic wastes. Hydrochloric Acid (HCl, 36%) and Polyvinyl alcohol (PVA) was purchased from Merck Inc. Aqueous solution of ammonia (30 wt.%), Deionized water, Hexadecyl trimethylammonium bromide (CTAB, 99.5%), zinc chloride ($ZnCl_2$, 99.90%), (N, N- Dimethylformamide (DMF, 99.98%) and potassium hydroxide (KOH, 98%) were supplied from Sigma-Aldrich and used without further purification.

2.2. Synthesis of carbon powder and activation procedure

2 g of each precursor (back tea or carbonated soft drink) was separately stirred with 0.5 mL of aqueous ammonia and 0.06 g of CTAB for 4 h. The resulting mixture was filtered and then poured into a Teflon-lined autoclave, which was then placed in an oven for 5 h at 270 °C. The resulting powder was washed twice with deionized water and twice with ethanol, and then it was centrifuged and dried in air at 50 °C for 12 hours. The resulting powder is arbitrarily called the "raw carbon particles" and abbreviated (RCP).

Two-step activation of RCPs with $ZnCl_2$ and then with KOH was applied, to do this first, 1 g of resulted in RCP was mixed with $ZnCl_2$ with the mass ratio of RCP/$ZnCl_2$=1/1 and 50 mL of H_2O. The resulting suspension was kept under stirring for 2 h at 50°C then it was dried in the oven for a day at 90 °C. The resulting sample was stirred with KOH with the mass ratio of RCP/ KOH =1/1 and 30 mL of water in the second step of the activation. The mixture again was stirred at 50°C for 2 h and then dried for a day in the oven at 90 °C. The resulting sample was then placed in a furnace adjusted to raise the temperature

with a rate of 5°C/min from 25 °C to 350 °C and then from 350 °C to 800 °C. The temperature rises halted twice once at 350 °C and once at 800 °C each for 2 h. Finally, the activated samples were completely washed with an aqueous solution of HCl (1 M) and deionized water, and then they were centrifuged and dried at 50˚C for 12 hours. Afterward, the samples were placed in a crucible and ground in mortar manually and with the aid of an electric grinder for about 1 h.

2.3. Synthesis of AC/PVA mixed matrix membrane

To synthesize the casting solution of MMMs, a polymeric solution with a concentration of 44.44 g.lit^{-1} of PVA in water was produced by dissolving 4 g of PVA in 90 ml of deionized water at 60 °C for 4 h. Three separate suspension samples with loadings of 5, 10, and 20 wt.% of AC powder in deionized water were produced followed by vigorous stirring for 2 h. The resulting suspension was separately added to the PVA solution then successive operations of 15 min of sonication and 30 min of stirring were applied to the MMM solution (3 cycles). The resulting samples were aged for 2 h for bubble removal. For the preparation of MMMs, a non-woven polyester fabric was supplied and used as the substrate and mechanical support of MMM. A surface of 10×10 cm^2 of fabric was stuck to a flat glass sheet with hydrophobic plastic sticks around the whole sheet. The dip coating method was used to coat the fabric support: the glass sheet covered with fabric was gently immersed into a bath of PVA/AC solution vertically and remained there for 3 seconds then gently removed from the bath. Then the glass was placed in a clean environment in the lab and held its position for 48 h for solvent (water) evaporation. The coated fabric which is our targeted MMM was removed from the glass and maintained in a clean environment to be evaluated in permeation experiments. The code names of the prepared samples in this study along with the preparation parameters are provided in Table 2.

Table 2
The code names of synthesized and modified MMMs with different waste precursors and activation chemicals

Code names of membranes	Precursor for AC	AC loading
Tea-AC/PVA-0.5	Black tea	0.5 g (5 wt.%)
Tea -AC/PVA-1	Black tea	1 g (10 wt.%)
Tea -AC/PVA-2	Black tea	2 g (20 wt.%)
Coke-AC/PVA-0.5	Carbonated soft drink	0.5 g (5 wt.%)
Coke-AC/PVA-1	Carbonated soft drink	1 g (10 wt.%)
Coke-AC/PVA-2	Carbonated soft drink	2 g (20 wt.%)

2.4. CO_2 and CH_4 permeance measurements

The permeances of CO_2 and CH_4 were measured using a flat PTFE membrane module equipped with a bubble flowmeter. The CO_2 and CH_4 gas capsules containing gases with 99.99% purity were used as the feed of membranes (Fig. 1).

The permeances of CO_2 and CH_4 were calculated based on the following formula:

$$P_i = \frac{Q_i}{A(p_{f_i} - p_{p_i})} \times 10^{-6} \quad (1)$$

where P_i is the symbol for permeance (GPU) of gas i, Q_i is the volumetric flowrate of gas i in the permeate stream (cm^3(STP) s^{-1}), A is permeable membrane area (cm^2), and p_{pi} is permeate side pressure and p_{fi} is feed side pressures of gas i (cmHg).

Dividing the permeance of a more permeable penetrant (A) to that of a less permeable penetrant (B) leads to the definition of the ideal selectivity $\alpha_{A/B}$ by the following formula:

$$\alpha_{A/B} = \frac{P_A}{P_B} \quad (2)$$

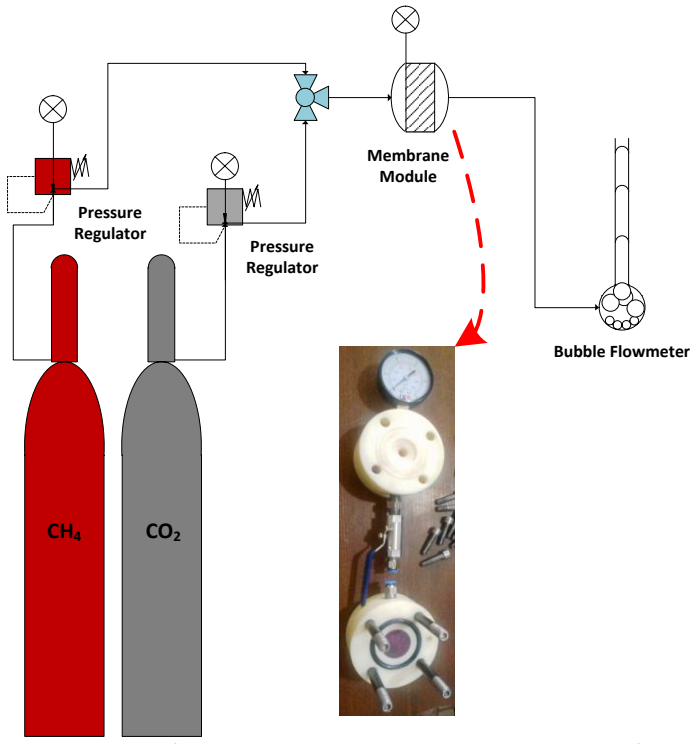

Fig. 1. Schem and image of applied gas permeation apparatus with an embedded image of the utilized membrane module.

2.5. Characterization

To investigate the morphology of the cross-section of membranes in two different levels of magnifications together with the surface morphology of the membranes, a scanning electron microscope (SEM) (TESCAN-MIRA3) at a voltage of 10 kV was used. The FT-IR (IRAffinity-1S, Shimadzu) spectra for the identification of new formation of groups at the prepared membrane's surface with an average of 8 scans in the range of 400-4000 cm^{-1} at a resolution of 5 cm^{-1} were applied. The attenuated total reflection (ATR) sampling technique was applied to the record of all spectra for review. The volumetric measurement approach at pressure up to 1 bar and the temperature of 77 K was adapted to determine the adsorption isotherms for all samples. About 0.15 g of each considered sample was separated and applied in the determination of each isotherm at 70 °C for about 120 min of vacuum was exerted on every membrane before the test for the sake of confidence that the pores of the sample are empty. The BET method has been used for the calculation of the BET area of membranes using obtained data in the range of $0.02<P/P_0<0.2$ from the corresponding isotherm. The pore size profile of membranes was measured following the density functional theory using specific software provided by Micrometrics (ASAP 2020). The appropriateness of fit with the adjustment parameter of 0.01 was selected as a reference point for the simulation.

3. Modeling and Economic Evaluation

The solution-diffusion mechanism which is an established and widely trusted model for defining the permeation through the membrane was regarded as the foundation of the modeling in this study. If the eq. (1) is expressed with more detail for j numbers of penetrants, and the resulting equation become as follows:

$$J_j = \frac{y_j \dot{V}}{A} = P_j[p_f x_j - p_p y_j] \quad (3)$$

For a two-component feed (e.g. CO_2 and CH_4) above equation, the above equation can be turned into the following equation using division:

$$\frac{y_1}{y_2} = \alpha \frac{p_f x_1 - p_p y_1}{p_f x_2 - p_p y_2} \quad (4)$$

where subscript (1) and (2) are related to the CO_2 and CH_4 respectively and α is the CO_2/CH_4 selectivity of the membrane.

Rearranging Eq. (4) yields a quadratic algebraic equation:

$$\left(\frac{p_p}{p_f}+\alpha\left(p_f-p_p\right)\right)y_1^{\,2}+\left(\alpha x+1-x-\frac{p_p}{p_f}-\alpha\left(p_f-p_p\right)\right)y_1-\alpha x_1=0 \quad (5)$$

Solving equation (5) gives y_1 and thereafter the flux through the membrane (J). However, due to the limitation of the effective surface area of a flat membrane module, the total flux (J_{total}) trough membrane is calculated based on the product of flux through a single membrane (J_{single}) and the number of modules determined by the user (n) in the user-interface of the model:

$$J_{total}=nJ_{single} \quad (6)$$

As it is obvious the membrane system configuration for the actual separation of CO_2 from CH_4 requires showing both high purity and at the same time high recovery for more selective gas. Currently, to reach both performance criteria for a separation system, multistage membrane processes with or without recycling of permeate or retentate are numerously reported in which the majority of the modules were hollow fiber to achieve higher surface area. Based on our knowledge of previous work on modeling and simulation of the membrane separation system, we believe that with a high-performance CO_2 selective membrane, which shows high permeance and selectivity, it is possible to design a simpler system configuration with a series of flat sheet modules. The proposed system configuration in this work is presented in Fig. 2.

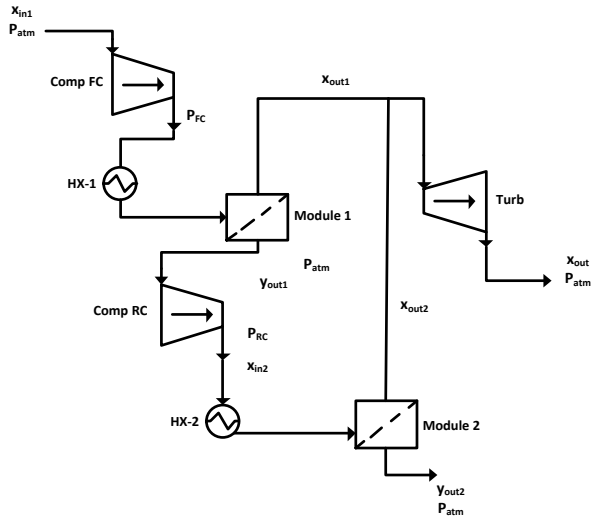

Fig. 2. The schematic diagram of the designed two-stage membrane separation configuration.

As can be seen, the proposed system configuration is a double-stage membrane system without recycling and with cooling after the compression of feed in each stage. The connection between the two stages of gas separation is based on the following basic conservation of mass equations:

$$F_{in2}=\dot{V}_{out1} \quad (7)$$

$$x_{CO_2in2}=y_{CO_2out1} \quad (8)$$

$$x_{CH_4in2}=y_{CH_4out1} \quad (9)$$

To define the evaluation parameters for the performance of the whole membrane separation system we have to define the parameters related to the single membrane module and expand them to the whole system. The performance parameter for s single module is given by: (The definition of the parameters and symbols are provided in nomenclature at the end of the text).

$$purity_{CO_2}=y_{CO_2out2}\times 100 \quad (10)$$

$$Recovery_{CO2}=\frac{\dot{V}_{out2}\times y_{CO_2out2}}{F_{in1}\times x_{CO_2in1}}\times 100 \quad (11)$$

$$Purity_{CH_4}=\frac{F_{out1}x_{CH_4out1}+F_{out2}x_{CH_4out2}}{F_{out1}+F_{out2}}\times 100 \quad (12)$$

$$Recovery_{CH_4}=\frac{F_{out1}x_{CH_4out1}+F_{out2}x_{CH_4out2}}{F_{in1}x_{CH_4in1}}\times 100 \quad (13)$$

$$I_{GP}=Purity_{CO_2}+Recovery_{CO_2}+Purity_{CH_4}+Recovery_{CH_4} \quad (14)$$

The I_{GP} is defined as the global index of separation performance of the system. This parameter can be used either in the optimization of the performance of the system or in the sensitivity analysis of the system. The importance of the IGP in the evaluation of the performance of a separation process is related to the fact that this factor summarizes the production rate and purity degree of the system. Obviously, there is a constant trade-off between these two parameters, hence it is critical to find the optimum point of this trade-off which maximizes the IGP factor.

For the economic evaluation of the proposed system, an adopted approach from the work of Hao et al. for upgrading low-quality natural gas was selected. However, the parameters of the original approach were modified based on the properties of the current work by the inclusion of a turbine for possibly utilizing the effluent energy of high-pressure gas and intercooler exchangers for temperature reduction of feed gases.

The total costs of the proposed system configuration involve capital costs, operating costs, and costs related to the loss of mass in permeate streams [43]. That is given by:

$$TC=\frac{CC+OC+LSC}{\dot{V}_T} \quad (15)$$

$$\dot{V}_T=\dot{V}_D\times OSF\times 365 \quad (16)$$

$$LSC=C_{LS}\dot{V}_{LS}H_V \quad (17)$$

$$\dot{V}_{LS}=\dot{V}_{out}\times y_{CH_4out2}\times OSF\times 365 \quad (18)$$

The capital costs mostly comprise fixed costs which are related to the cost of purchasing the equipment (membrane modules, compressors, turbine, and heat exchangers, neglecting the inexpensive piping costs). All of the cost data are referred to the 2018 indexes of CEPCI. The start-up and contingency costs are also included in fixed cost estimation:

$$CC=PI/t_f \quad (19)$$

$$PI=FI+SC \quad (20)$$

$$SC=OC/t_{start} \quad (21)$$

$$FI=BPC+PC \quad (22)$$

$$PC=0.2\times BPC \quad (23)$$

$$BPC=1.12\times FC \quad (24)$$

$$FC=MEC+TUC+HEC+COC \quad (25)$$

$$MEC=2\times A_{mem}Z_{mem} \quad (26)$$

$$TUC=(603/397)(0.03235\times WT^3-0.2818\times WT^2+0.9364\times WT+0.5252)\times 10^6 \quad (27)$$

$$HEC=(603/397)(5.034\times 10^{-6}\times AHE^4-2.49\times 10^{-4}\times AHE^3+4.37\times 10^{-3}\times AHE^2-0.02876\times AHE+0.2546)\times 10^6 \quad (28)$$

$$COC=COC_{FC}+COC_{RC} \quad (29)$$

$$COC_{FC}=(603/397)(-1.044\times 10^{-7}\times WFC^2+1.126\times 10^{-3}\times WFC+0.2076)\times 10^6 \quad (30)$$

$$COC_{RC}=(603/397)(-8.061\times 10^{-8}\times WRC^2+2.475\times 10^{-4}\times WRC+0.06865)\times 10^6 \quad (31)$$

The second most involved cost in capital costs estimation is operating costs. These costs are the current and ongoing costs of the system. The operating costs in this work involved utilities, replacement of membranes, labor, maintenance, and insurance costs.

The operating costs are expressed by the following relationships:

$$OC = IC + MC + LC + MRC + UC \tag{32}$$

$$IC = 0.015 \times CC \tag{33}$$

$$MC = 0.05 \times CC \tag{34}$$

$$LC = DLC + ILC \tag{35}$$

$$DLC = 24 \times 365 \times OSF \times n_{LAB} \times Z_{LAB} \tag{36}$$

$$ILC = 1.15 \times DLC \tag{37}$$

$$MRC = (A_{mem} Z_{mem}) / t_{mem} \tag{38}$$

$$UC = C_{ELEC} + C_{REF} \tag{39}$$

$$C_{ELEC} = 3600 \times 24 \times 24 \times Z_{ELEC} (WFC + WRC - WT) \times OSF \tag{40}$$

$$C_{REF} = 3600 \times 24 \times 365 \times Z_{REF} (\dot{V}_{FC} + \dot{V}_{RC}) \times OSF \tag{41}$$

To calculate the properties of compressors, turbines, and heat exchangers in the above equations, it is needed to utilize some axillary equations. For the first compressor and the first heat exchanger, we have:

$$Q_{FC} = 3 \times \dot{n}_{feed} \times c_{pfeed} (T_{hotFC} - T_{coldFC}) \tag{42}$$

$$AHE_{FC} = \frac{Q_{FC}}{U \times \Delta T_{FC}} \tag{43}$$

$$\Delta T_{FC} = \sqrt[3]{\left(\theta_{1FC} \times \theta_{2FC} \times \frac{\theta_{1FC} + \theta_{2FC}}{2} \right)} \tag{44}$$

$$\theta_{1FC} = (T_{hotFC} - T_{outREF}) \tag{45}$$

$$\theta_{2FC} = (T_{coldFC} - T_{inREF}) \tag{46}$$

$$T_{hotFC} = (T_{coldFC} + 273.15) \left(1 + \frac{1}{\eta} (r_{PFC}^{(\gamma-1)/\gamma} - 1) \right) - 273.15 \tag{47}$$

$$r_{PFC} = \sqrt[3]{\left(\frac{P_{outFC}}{P_{atm}} \right)} \tag{48}$$

$$WFC = 3 \times \frac{\dot{n}_{feed}}{\eta} \frac{\gamma - 1}{\gamma} R (T_{coldFC} + 273.15) (r_{PFC}^{(\gamma-1)/\gamma} - 1) \tag{49}$$

Similarly, for the first compressor and the first heat exchanger, we have:

$$Q_{RC} = 3 \times \dot{n}_{Rfeed} c_{PRfeed} (T_{hotRC} - T_{coldRC}) \tag{50}$$

$$AHE_{RC} = \frac{Q_{RC}}{U \times \Delta T_{RC}} \tag{51}$$

$$\Delta T_{RC} = \sqrt[3]{\left(\theta_{1RC} \times \theta_{2RC} \times \frac{\theta_{1RC} + \theta_{2RC}}{2} \right)} \tag{52}$$

$$\theta_{1RC} = (T_{hotRC} - T_{outREF}) \tag{53}$$

$$\theta_{2RC} = (T_{coldRC} - T_{inREF}) \tag{54}$$

$$T_{hotRC} = (T_{coldRC} + 273.15) \left(1 + \frac{1}{\eta} (r_{PRC}^{(\gamma-1)/\gamma} - 1) \right) - 273.15 \tag{55}$$

$$r_{PRC} = \sqrt[3]{\left(\frac{P_{outRC}}{P_{atm}} \right)} \tag{56}$$

$$WRC = 3 \times \frac{\dot{n}_{Rfeed}}{\eta} \frac{\gamma - 1}{\gamma} R (T_{coldRC} + 273.15) (r_{PRC}^{(\gamma-1)/\gamma} - 1) \tag{57}$$

The combined area of heat exchangers is calculated by summation of the surface area of each exchanger:

$$AHE = AHE_{FC} + AHE_{RC} \tag{58}$$

The work that is produced by the turbine is calculated by:

$$WT = \frac{\dot{n}_{Tfeed}}{\eta} \frac{\gamma - 1}{\gamma} R (T_{inT} + 273.15) \left(\frac{P_{atm}}{P_{inT}} \right)^{(\gamma-1)/\gamma} \tag{59}$$

The pressure imposed on the feed of each stage is dependent on the other stage and is also determined by the corresponding compressor and thermodynamics limitations. The pressure of the entering stream to the system is atmospheric and the pressure of each stage is variable depending on the technical calculations and mathematical limitations.

Because one of the most encountered mixtures of CO_2 and CH_4 in the industry especially in Middle East countries is natural gas feed to the sweetening plants, the case to consider for simulation in this study is a feed to a natural gas sweetening plant. The usual CO_2 content of natural gas in underground reservoirs is 10 vol.% to 20 vol.%, hence we consider a CO_2:CH_4 composition of 15:85% with an average feed flow rate of about 1000 m^3 STP/h. In the considered case, the feed is assumed to be a mixture of gas of CH_4 and CO_2, which is a roughly correct assumption for the natural gas composition used in the simulation. The performance and economic evaluations of the proposed system configuration were performed by a series of sensitivity analyses and the optimized condition was determined based on the results of those analyses. These evaluations for the CO_2/CH_4 separation process were performed in the MATLAB environment and the decision for determination of the best separation performance among systems equipped with different membranes has been made based on the calculated parameters such as purity of gases, recovery of gases, and IGP factor. For the economic evaluation of the process, the calculated parameters such as operating costs, capital costs, loss costs, and total costs were utilized for the judgment of the most economically attractive set of operating parameters for the best-performing membrane determined by performance evaluation.

The parameters defined in the modeling of membrane system configuration are shown in Table 3.

We entered the selectivities of all seven membranes tested in technical evaluation, as a vector in MATLAB, then we wrote a quadratic algebraic equation related to equation (6) to calculate the roots which are permeated CO_2 composition exiting stage 1. We also programmed the two formulas based on equation (3) to calculate the CO_2 and CH_4 permeate fluxes exiting stage 1. Then the selectivities of seven membranes as a vector and the quadratic algebraic equation related to equation (6) for stage 2 were entered in MATLAB similar to what was done for stage 1. Then the constants presented in Table 3 were entered and the formula from (8) to (60) was entered in the MATLAB environment for the calculation of technical and economical parameters introduced in the text. It is important to keep in mind that, for economical evaluations, only the best-performed membrane in the technical evaluation was selected for sensitivity analysis of the economic evaluation part of the work (See supplementary MATLAB file).

Table. 3
The main constant and variable parameters are defined in the techno-economical analysis.

Parameter	Value	Unit	Ref.
CO_2 permeance (first stage)	From 41 to 62	GPU	From Experiments
CO_2 permeance (second stage)	From 22 to 33	GPU	From Experiments
CO_2/CH_4 selectivity	From 13.33 to 23.21	-	From Experiments
C_p/C_v (γ)	1.35	-	[44]
efficiency (η)	0.7	-	[44]
Ref. gas temperature (T_{cold})	25	ºC	[44]
Inlet temp. of cooling water (T_{in})	5	ºC	our own choice
Outlet temp. of cooling water (T_{out})	15	ºC	our own choice
Overall heat transfer coefficient (U)	0.6	$kW/m^2 \cdot K$	[45]
Specific heat capacity (C_{PFEED}, CP_{RFEED})	37	kJ/kmol·K	[45]
CO_2 composition in feed	0.15	-	our own choice
Feed pressure	20	atm	our own choice
Second-stage feed pressure	5	atm	our own choice
Area of a single module stage 1	0.13	m^2	From Experiments
Area of a single module stage 2	0.19	m^2	From Experiments
Predicted start-up time	0.5	year	[46]
Predicted plant lifetime	25	year	[46]
On-stream factor (OSF)	0.95	-	[46]
Price of Electricity (Z_{elec})	2×10^{-5}	$/kJ	[45]
Price of Refrigeration (Z_{ref})	4.5×10^{-6}	$/kJ	[45]
Price of Membrane (Z_{mem})	From 24 to 39	$/$m^2$	our own experience
Salary of Operators (Z_{lab})	2.5	$/h	our own choice
Number of operators (n_{lab})	3	person	our own choice
Membrane lifetime (t_{mem})	2, variable	y	our own choice
Heating value (H_V)	4.2×10^{-4}	kJ/m^3	[45]
Loss of Methane value (C_{LS})	2×10^{-5}	$/kJ	[43]

4. Results & Discussions

4.1. Result & Discussion of Experimental Investigations

4.1.1. SEM

The SEM micrographs from the AC particles synthesized from two different precursors are provided in Fig. 3a and b.

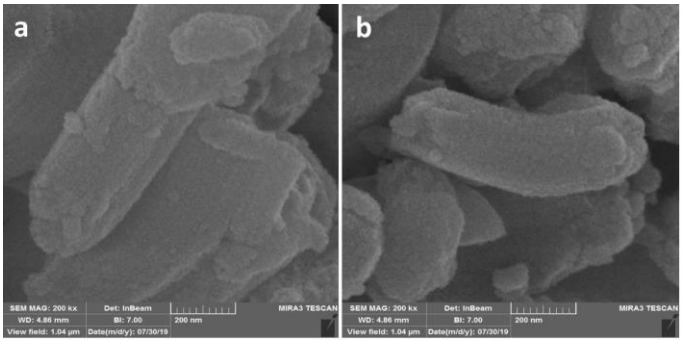

Fig. 3. SEM micrograph of activated carbon samples synthesized by a) tea waste and b) coke waste

As can be seen, the AC particles in the two images have a width of about 200 nm and a length of about 1 µm. These AC particles with the size indicated in SEM images are not suitable to be used as fillers in ultra-thin mixed matrix membranes or thin composite membranes. This is simply because the AC particles can not be distributed properly in the selective layer and the chances of the creation of a defective selective layer rise. Therefore a relatively thick selective layer would be proper for the utilization of these AC particles. Although wastes of tea resulted in larger particles than coke wastes, however, the difference between the sizes of particles in the two images is not significant. Despite having a large size, these particles show proper porosity observable in SEM images. As can be seen, the surface of AC particles is not smooth and there is roughness observable on them which is the result of small pores at the surface of these particles.

The cross-sectional SEM micrographs of all fabricated membrane samples are provided in Fig. 4a-f.

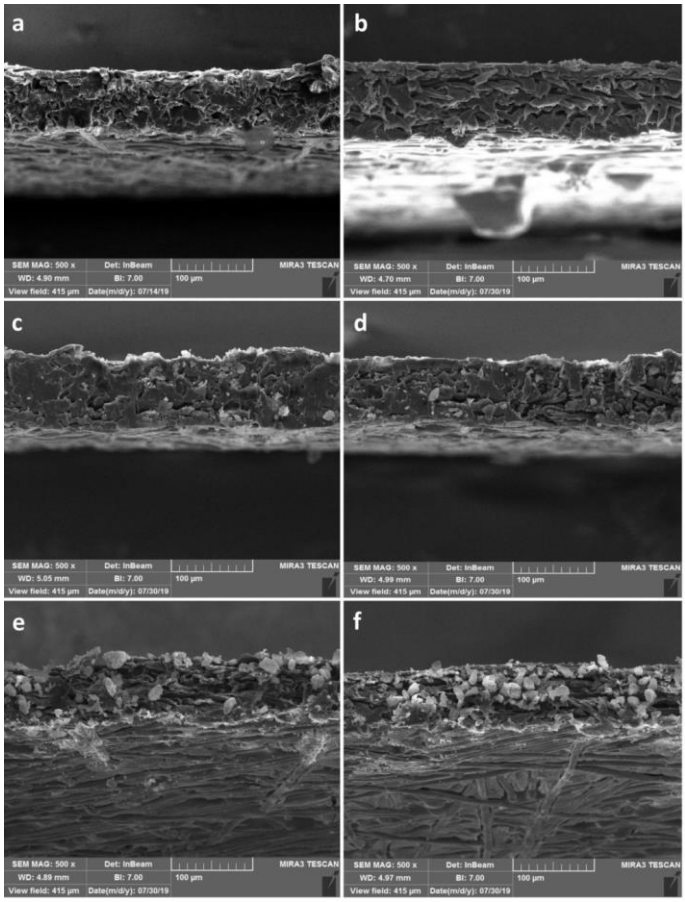

Fig. 4. SEM images from the cross sections of a) Tea-AC/PVA-0.5, b) Coke-AC/PVA-0.5, c) Tea-AC/PVA-1, d) Coke-AC/PVA-1, e) Tea-AC/PVA-2 and f) Coke-AC/PVA-2.

As can be seen in this figure, the thickness of the membrane and nonwoven polyester substrate is about 80-100 µm for all membranes synthesized in this work. The reason as explained before is related to the size of AC particles which makes this impossible to fabricate this mixed matrix membrane. At top of the membranes, there is no observable distinct selective layer which is the result of the utilization of nonwoven polyester as a substrate for enhancement in the mechanical stability of the resulting membranes and to prevent the formation of a very thick and dense PVA selective layer. As can be observed, with the increase in the loadings of AC particles in PVA solution, the observability of the particle at the cross-section increases. The aggregated and single particles at the loading of 0.5 g are rarely observed at the cross sections of Tea-AC/PVA-0.5 and Coke-AC/PVA-0.5 samples (Fig. 4 a and b) while they are present at the cross sections of Tea-AC/PVA-1 and Coke-AC/PVA-1 samples (Fig. 4 c and d) and Tea-AC/PVA-2 and Coke-AC/PVA-2 samples (Fig. 4e and f) with loadings of 1g and 2 g respectively.

The surface SEM images of prepared membranes are presented in Fig. 5 a-f.

The nonwoven fibers of the polyester substrate are detectable in all subsections of Fig. 5. Some voids can be observed at the surface of most of the membranes which are related to the penetration of PVA/AC solution through the fibers of polyester. However, because the membranes have fairly high thickness compared with conventional MMMs, the penetration of a percentage of coating solution in the substrate should not create a defective layer. Another point worth mentioning is that as the concentration of AC powder increases in the PVA solution because the viscosity of the coating solution partially increases, the penetration of the coating solution in the fibers of the substrate becomes limited. Hence one can see a smoother surface in Fig 5. e and f when compared with Fig. 5 c and d, the then again smoother surface was observed when compared all mentioned subfigures with Fig. 5 a and b.

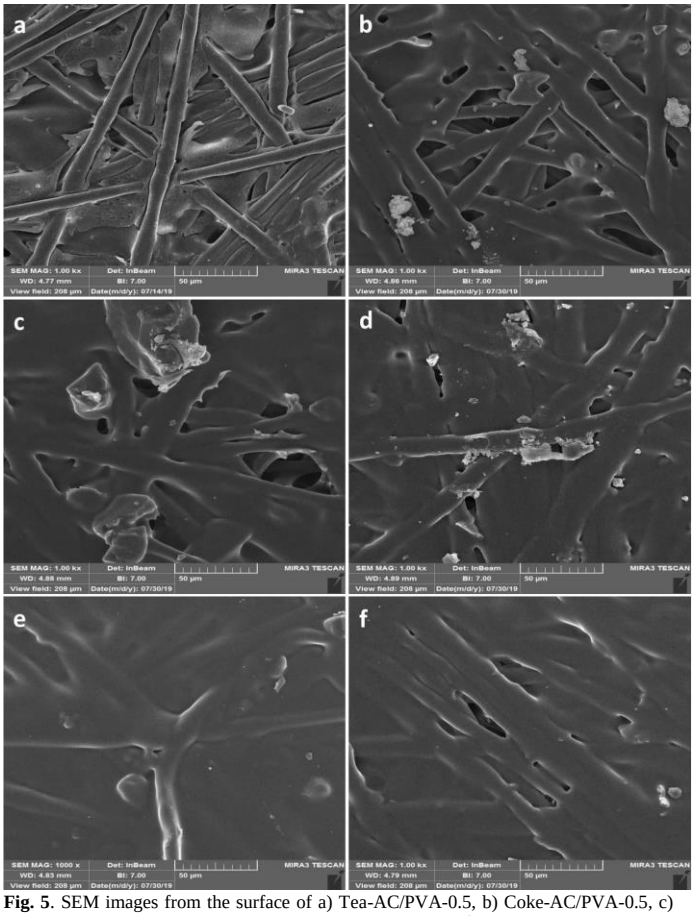

Fig. 5. SEM images from the surface of a) Tea-AC/PVA-0.5, b) Coke-AC/PVA-0.5, c) Tea-AC/PVA-1, d) Coke-AC/PVA-1, e) Tea-AC/PVA-2 and f) Coke-AC/PVA-2.

4.1.2. FTIR

The FTIR spectra of prepared membrane samples in this work are merged and shown in one figure (Fig. 6).

As can be seen, the common spectra of all samples from the right to left are at wavenumbers of 1027, 1515, 1550, 1620, 2170, 2855, 2926, and 3450cm^{-1} which are respectively related to the stretching vibration of C-O in saturated alcohols or the stretching vibration of C–O–C in furans (1027 cm $^{-1}$), the emission of H_2O (1515 cm $^{-1}$), the hydrates of zinc chloride on exposure to the H_2O molecule (1550 cm $^{-1}$), the vibration of C=C in the carbon ring (stretching), (1620 cm $^{-1}$), the vibration of C=O indication the scission of the vinyl external linkages (2170 cm $^{-1}$) (stretching), the same but symmetric vibration of C-H (2855 cm^{-1}) and finally the asymmetric stretching vibration of C-H (2926cm^{-1}). Except for the peak at 1515 cm^{-1}, which is related to the functionalization of samples with $ZnCl_2$, the other mentioned peaks are characteristics of PVA. The peak near 3450 cm^{-1} is attributed to the stretching vibration of O-H which belongs to H-bonded phenolic OH. This peak is most probably the result of the incorporation of KOH in the functionalization of ACs. The peaks are all common in all synthesized samples meaning that all of the synthesized membranes are properly activated with $ZnCl_2$ and KOH agents.

4.1.3. N_2 Adsorption-Desorption, DFT, BET

The N_2 ads.-des. isotherms and DFT PSD of MMMs are presented in Fig. 7a-d.

In Fig. 7a, with the increase in the concentration of AC particles in the matrix of PVA, the sorption capacity of the membrane increases significantly. This was an anticipated result because the higher loadings of AC particles provide more pores for the sorption of gases. Moreover, the isotherms of samples prepared with ACs from Tea wastes are similar to types I and IV of isotherms based on the BDDT classification system which demonstrates that the gas molecules adsorbed in pores in mostly micropores. The fact that the isotherms at extremely small partial pressure (P/P_0<0.05) are not completely vertical demonstrates the existence of meso-sized pores in the membranes. This is in accordance with the result reported by Malhotra et al. [47]. The DFT PSD of samples demonstrates that the very high population of the pores are micropores and to some extent in a mesoporous regime which confirms the result of the N_2 adsorption analysis. The mean pore size of Tea-AC/PVA samples is provided in Table 4.

For the case of membranes synthesized with AC from coke wastes, the behavior of N_2 adsorption isotherms and DFT PSD are very similar to those synthesized with AC from tea wastes except for observed hysteresis in isotherms. The hysteresis observed in N_2 adsorption isotherms of Coke-AC/PVA samples (Fig. 7c), is most probably related to the relative abundance of micropores in the structure of ACs in these membranes which partially prevents the evacuation of micropores during pressure reduction in desorption process. This can be deducted to some extent from the DFT PSD of Coke-AC/PVA samples (Fig. 7d) when compared with Fig. 7b. As can be seen the relative abundance of particles with sizes larger than 4 nm is noticeably lower for Coke-AC/PVA samples compared with Tea-AC/PVA samples which mean the larger population of micropores in Coke-AC/PVA samples. This explanation is also backed up by the textural properties provided in the Table 4.

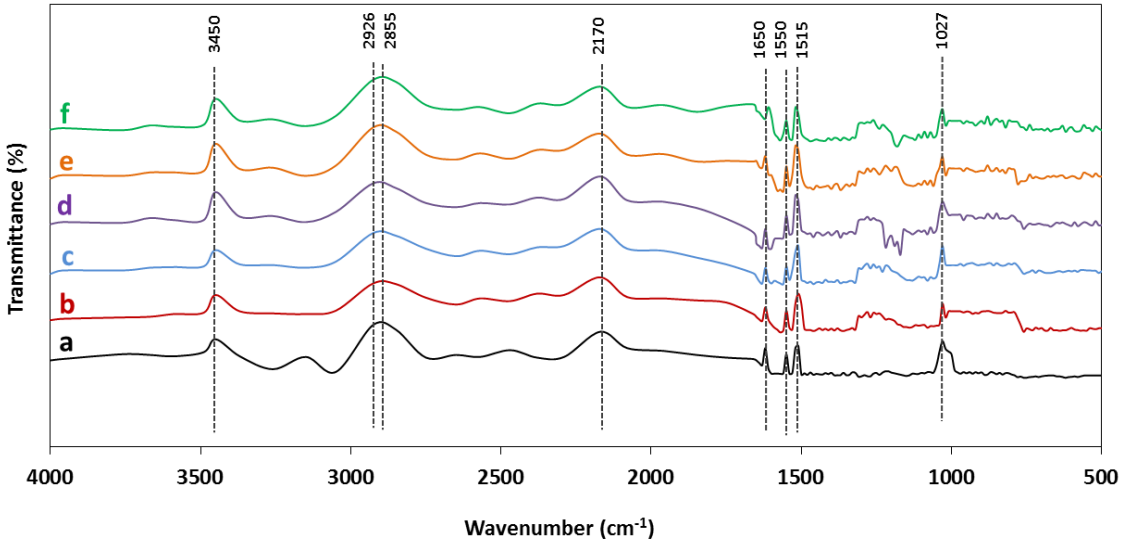

Fig. 6. The FTIR spectrum of a) Tea-AC/PVA-0.5, b) Coke-AC/PVA-0.5, c) Tea-AC/PVA-1, d) Coke-AC/PVA-1, e) Tea-AC/PVA-2 and f) Coke-AC/PVA-2.

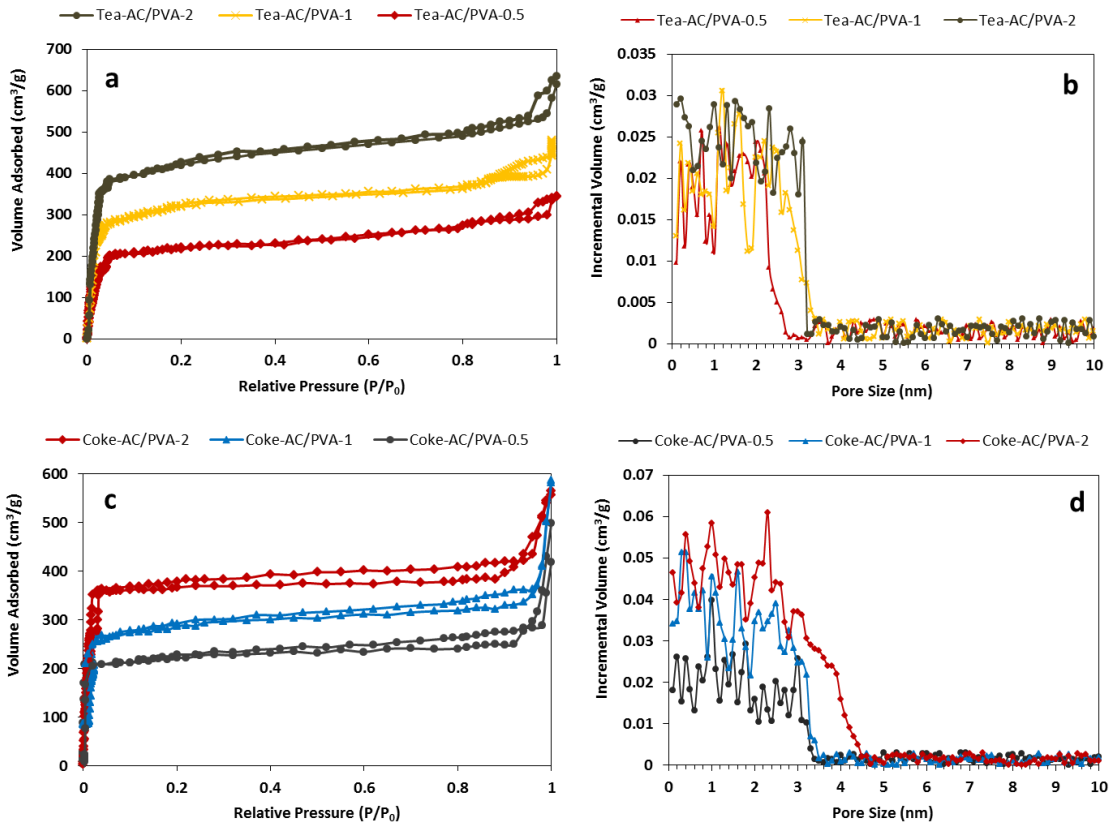

Fig. 7. a) N_2 ads.-des. isotherms and b) DFT PSD of Tea-AC/PVA group of membranes, c) N_2 ads.-des. isotherms and d) DFT PSD of Coke-AC/PVA group of membranes.

Table 4
Some textural properties were extracted from the adsorption analysis of the synthesized membranes.

Code names of membranes	BET (m^2/g)	Volume of pores (mL/g)	pore size (mean) (nm)
Tea-AC/PVA-0.5	433	0.368	2.4
Tea -AC/PVA-1	625	0.589	2.5
Tea -AC/PVA-2	873	0.779	2.6
Coke-AC/PVA-0.5	398	0.351	2.4
Coke-AC/PVA-1	602	0.555	2.5
Coke-AC/PVA-2	846	0.759	2.8

4.1.4. Permeation Examinations

The permeation test results (CO_2 and CH_4 permeances and CO_2/CH_4 ideal selectivity) at a temperature of about (30 ˚C) and feed pressure of 20 bar are presented in Fig. 8.

It is observed that with the increase in the loading of ACs in the matrix of PVA, in all synthesized MMMs, the CO_2 and CH_4 permeances increase notably. The CO_2 permeance increase is more significant than CH_4 permeance. This is for several reasons:

1- The molecular etic diameter of CH_4 (0.38 nm) is larger than the molecular diameter of CO_2 (0.33 nm), therefore as the loading of porous AC increases in the membranes the diffusion becomes easier for smaller molecules of CO_2 in the pores of AC compared with larger molecules of CH_4.

2- The affinity of ACs for the sorption of carbon dioxide is significantly larger than that for methane, this is mainly because of the noticeably higher CO_2 isosteric adsorption heat which covers the lower rate of adsorption of CO_2 compared with CH_4 and causes the higher sorption ability of membranes with higher loading of ACs [48].

3- In the presence of possible microvoids and defects at the particle-polymer interface, these voids favor the passage of smaller molecules and because the permeation experiments were conducted based on pure gas feed, the concentration and competition in diffusion were neglected.

4- The sorption of condensable CO_2 gas in the matrix of PVA leads to the swelling of the polymer structure due to plasticization. This increases the membrane FFV and finally the permeation flux of all penetrants, especially smaller molecules.

It is noteworthy that the membranes having ACs prepared with tea wastes showed superior separation performance compared with those prepared with coke wastes. The reason is related to the point that as was observed in N_2 adsorption analysis and BET results, the ACs synthesized with tea wastes show slightly higher sorption capacity of surface area, hence these enhanced properties favor the sorption of more soluble gas (CO_2) rather than less soluble gas (CH_4) leading to the observation of better CO_2/CH_4 separation performance for tea wastes originated membranes.

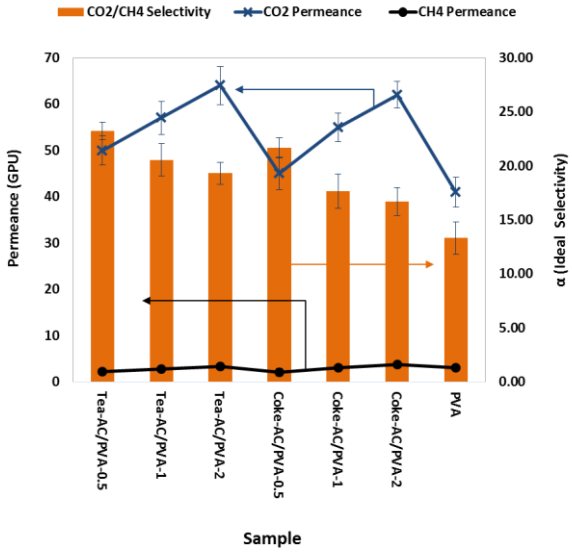

Fig. 8. CO_2 and CH_4 permeances and CO_2/CH_4 ideal selectivity of all synthesized membranes at the pressure of 20 bar and temperature of 30 ˚C.

The CO_2/CH_4 separation performance of all synthesized membranes is presented in Fig. 9. in comparison with Robeson's upper bound of 2008.

The CO_2/CH_4 separation performance of all AC/PVA MMMs is superior to the pure PVA membranes in terms of both permeance of CO_2 and permselectivity of CO_2/CH_4, however, the performance of MMMs is still well below the upper bound. The reason is that the improvement of the separation performance of MMMs with the aid of AC particle which is not an ordered microporous or mesoporous material with regular pore size has its limitations and it is not expected to observe a tremendous enhancement in the separation performance of AC/PVA membranes for gas separation applications when compared with pure PVA membrane.

4.2. Results and Discussions of Technical Evaluations

4.2.1. The permeate and retentate flow rates of the two-stage process

The simulated flow rates of permeated and rejected gases exiting the designed two-stage process for all membranes synthesized in this work are presented in Fig. 10.

The combined F_{out1} and F_{out2} streams are more than 800 m^3(STP)/h meaning that more than 80% of the whole feed ends up in the retentate stream. This percentage is comparatively higher for membranes with lower permeances. This result which was also observed in other works [38], is reasonable because the membranes in this work were all highly CO_2 selective with relatively low overall permeance and since the feed is 85% CH_4 and only 15% CO_2, the permeate stream has to be considerably low compared with retentate stream. It is also noteworthy that the difference between the retentate steam of the first step is significantly high which is due to the relatively low permeances of membranes and that results in the significant reduction of the stage cut of the 1st stage leading to the significant decrease in feed flow rate of the 2nd stage. This outcome forces the reduction of the pressure of the second stage compressor leading to the decline in driving force and permeances of the second stage.

4.2.2. The CO_2 and CH_4 Purities and Recoveries and IGP factor of membranes

The overall recoveries and purities of both gases along with the IGP factor for all membranes are presented in Fig. 11a and b.

From Fig. 10a it can be deduced that as the permeances of membranes decrease the recovery of CO_2 is affected significantly which is in agreement with the discussion in Fig. 10. Because the feed is mostly CH_4 and the gas permeances of membranes are relatively low, CO_2 recovery suffers the most. However, CH_4 recovery changes are mild and this is because very low permeances of membranes for this gas could not affect noticeably the very high CH_4 flow rates of retentates at each stage. Low recovery of CO_2 resulted in low purity of CH_4 at the retentate stream exit, however, the purity of CO_2 rise from 15% to over 96% for most of the membranes modeled. The IGP factors better show the performance of the membrane in a two-stage process (Fig. 11b). The ideal IGP factor value is 400 and as can be seen, Tea-AC/PVA-1 and Tea-AC/PVA-2 samples have the closest IGP values to this number compared with others. It is worth mentioning that as can be observed the IGP factor for pure PVA membranes is significantly lower than that for AC/PVA membranes. This demonstrates that the increase in permeance and CO_2/CH_4 selectivity of membranes because of the incorporation of AC not only boosts the separation properties of PVA membrane but also enhances the separation performance of the whole proposed system configuration. Moreover, as can be seen, the difference between the IGP of Tea-AC/PVA membranes and Coke-AC/PVA membranes is noticeable and it is more intense when compared with the permeation test results. This indicates that the as the separation stages increase the difference between the performance of membranes simulated in the membrane separation system increases because the partially purified permeate stream is used as the feed of the second stage and this leads to the observation of a larger separation performance difference in simulation between membranes which showed the milder difference in separation performance in experiments.

The dependency of purities, recoveries and IGP factors on the number of modules or whole membrane area of the system is presented in Fig. 12a-e.

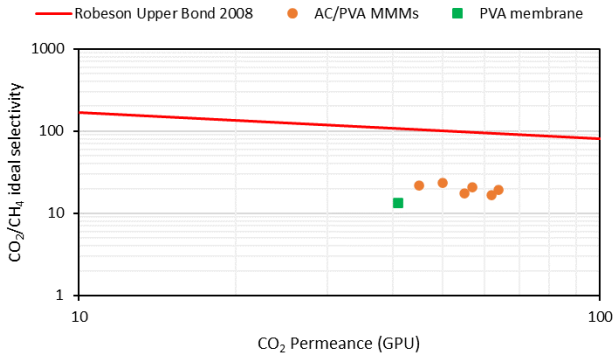

Fig. 9. The CO_2/CH_4 separation performance of all membranes in comparison with Robeson upper bound 2008.

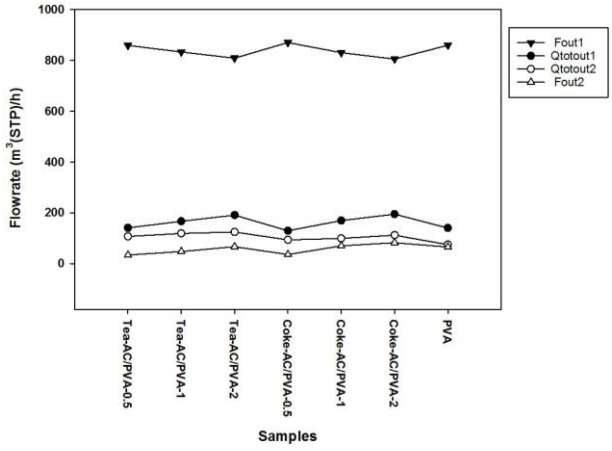

Fig. 10. The MATLAB simulated permeate and retentate flowrates of the two-stage process for all synthesized membranes

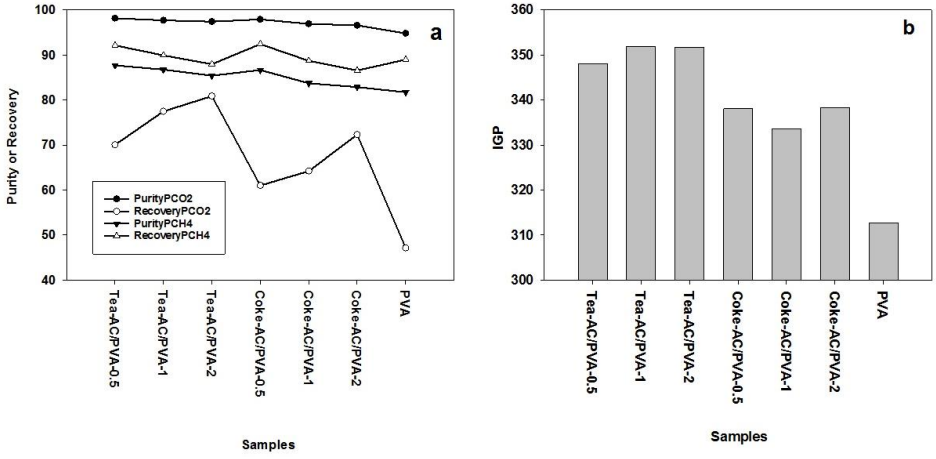

Fig. 11. a) Calculated overall CO_2 and CH_4 purity and recovery and b) IGP for all membranes.

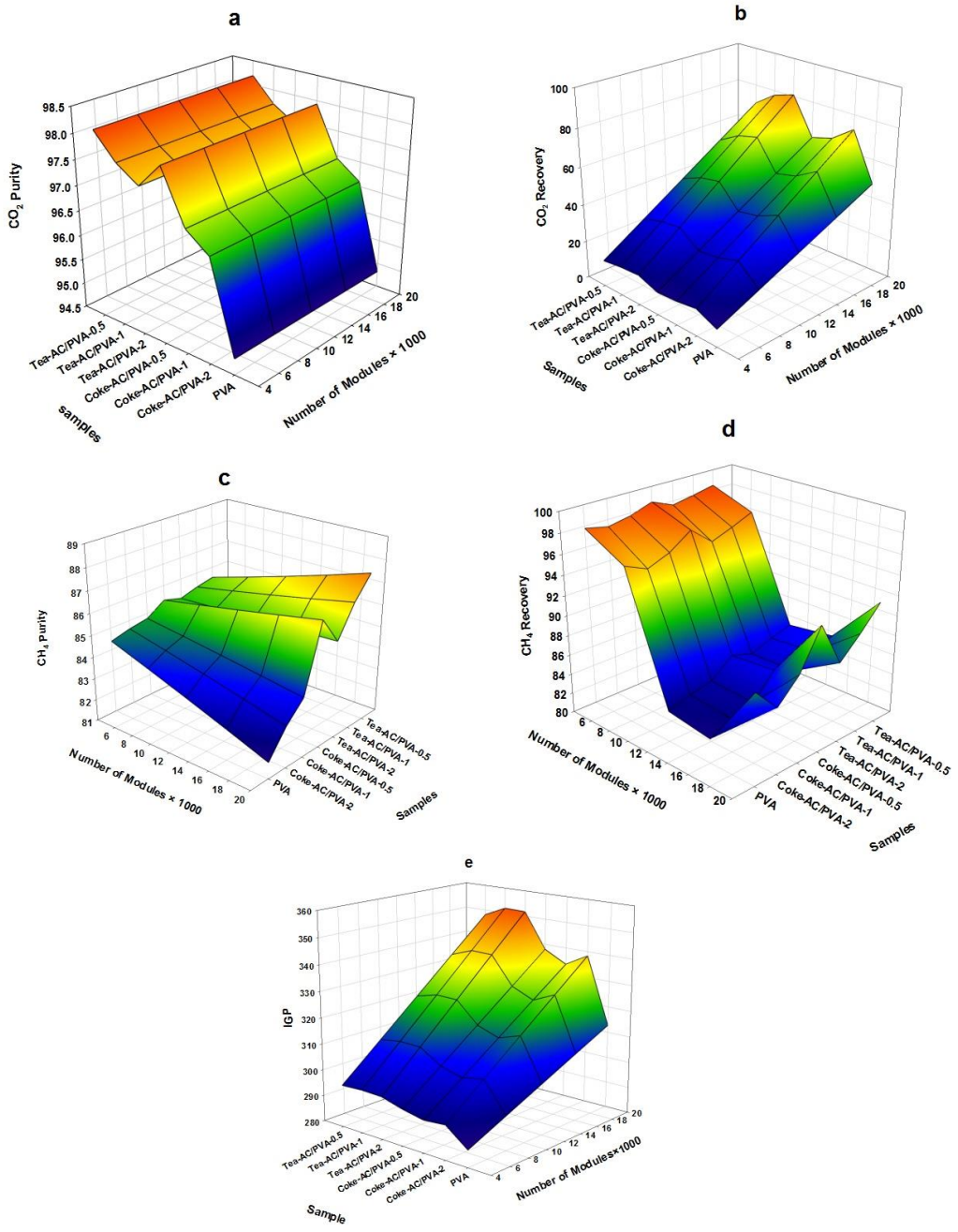

Fig. 12. Effect of the module number on a) purity of CO_2, b) recovery of CO_2, c) purity of CH_4, d) recovery of CH_4, and e) IGP factor for all synthesized membranes

The increased number of modules as can be seen has different effects on all of the factors investigated. The CO_2 purity shows independence to the number of modules while the CO_2 recovery increases with an increase in module numbers. This was predictable because the purity of CO_2 depends only on selectivity and because the selectivity does not change with increased membrane area and therefore permeate flux, constant CO_2 purity with increased membrane surface seems a logical outcome. For the CH_4 recovery, on the other hand, the membrane area and permeate flux are very influential because the recovery depends largely on the stage cut and permeation flux.

The CH_4 recovery decreases with an increase in the number of modules of the first stage and surface area. It is because, in contrast to other studies which were modeled and simulated hollow fiber modules, in this work, we modeled the flat sheet module that we used in our experiments. Therefore when the number of modules increases the driving force (concentration difference) between the feed side and permeate side does not change and remains constant but in hollow fiber module as the module length increase driving force of permeation decreases as a result of the decrease in concentration difference in feed (retentate) and permeate side. The approach we have taken in modeling in this work causes a nearly linear increase in permeate flow rate with the increase in the number of modules, this causes a partial decrease in retentate flow rate with the increase in the number of modules. For the second stage, because we did not change the number of modules at this stage, the changing trend in the retentate flow rate of this stage is conventional as it was expected. The increased number of modules in the first stage showed a considerable effect on the CH_4 composition of both stages leading to the observation of a decreasing trend for CH_4 recovery in simulation.

CH_4 purity shows an increasing trend for some samples and decreasing trend for others with the increase in the number of modules, CH_4 recovery shows a minimum for all samples and IGP shows an increasing trend with an increase in module numbers. This trend of change in purity and recovery of CH_4 with module number is related to the fact that the retentates of the two stages were mixed and because the purity of CH_4 in the first stage is lower than that of the second stage, therefore, mixing these two streams resulted in unpredictable outcome for CH_4 purity and recovery of the whole system with the increased membrane surface. However, in summary, for the case of IGP, the trend of change is similar to what was observed for CO_2 recovery because the changes in CO_2 recovery with the number of modules are huge compared with the change in the other three factors involved in IGP calculation. Hence it

can be concluded that the variation in CO_2 recovery has the most significant effect on the values of the IGP factor among all four factors calculated.

4.3. Results and Discussions of Economic Evaluations

4.3.1. Compressors vs. Turbine works and costs

For the economic evaluation of the process, the properties of the sample with the highest value of IGP (Tea-AC/PVA-1) were used.

In the first step of the economic evaluation of the process, we compared the number of works consumed by compressors and generated by a turbine with the increase in feed flow rate and then we compared the cost of the compressors and turbine together (Fig. 13a and b).

As can be seen in Fig. 13a, as the feed flow rates increase, the work produced by the turbine and consumed by compressors (combined) linearly increases. This was because of the linear dependency of works of these types of equipment with entering flowrates which are fractions of feed flowrate. The work consumed by two compressors is significantly larger than the work produced by the turbine, especially at larger flow rates. This means that for the process to become more economically attractive it is best to operate at smaller scales with lower flow rates. This is approved by results presented in Fig. 13b. As can be seen the cost of the turbine hugely rises while the cost of compressors increases slightly with the increase in flow rate. The cost of the turbine at a feed flowrate of 3000 m^3(STP)/h is about 1000 larger than the cost of both compressors combined meaning that from the economic point of view for this system it is extremely necessary to work at flowrates near 1000 m^3(STP)/h to limit the cost of the turbine.

4.3.2. Total costs, Capital costs, and Operation costs

For the system, the total cost per volume of the feed processed, the total cost per year, the capital cost per year, and the operating cost per year versus membrane lifetime at different flow rates are presented in Fig. 14 a-d.

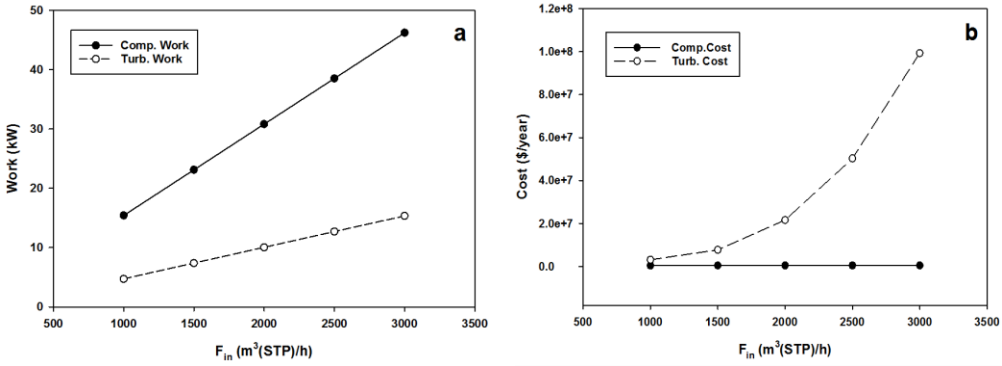

Fig. 13. a) Consumed compressors work and generated turbine work and b) cost of compressors and turbine

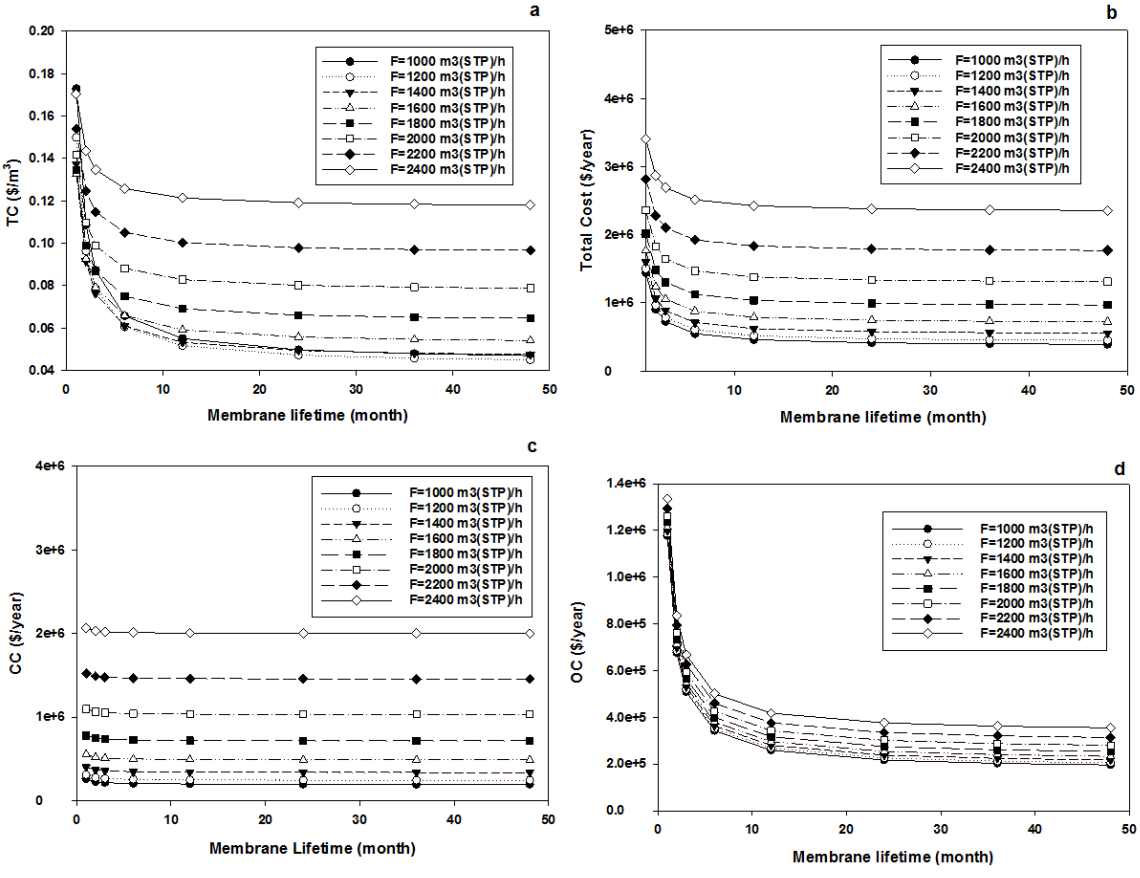

Fig. 14. a) TC, b) Total Cost, c) CC, and d) OC all versus membrane lifetime at different flowrates

In all four subsections of Fig. 14, as the average membrane lifetime increases, the total costs per volume of flowrate, total costs, capital costs, and operating costs decline at different rates. The membrane lifetime below 6 months causes a substantial increase in the total cost of the system. Hence the endurance of the membrane must be kept in mind when selecting or synthesizing a membrane for actual operation conditions because this factor can easily fail an economically attractive design if the selected membrane has a relatively short average lifetime. The lifetime of the membrane directly affects the membrane replacement costs (MRC) which is a noticeable percentage of the operating cost (OC) of the system at a low membrane lifetime. e.g. For a membrane with 4 years of lifetime, MRC is only about 0.1 of OC, however, if a membrane has a lifetime of a month MRC involves 0.84 of OC. The OC is only a part of CC, hence the change in OC which is very sharp does not significant effect on CC except for a very low membrane lifetime. It is noteworthy that when we compare the result of this work (Fig. 14a) with other published works [49, 50], the TC below 0.05 $/m^3 which was determined as the economically attractive value of the process was reached in this work for the sample investigated at for membrane lifetime over two years, meaning that some of the samples in this work show potential to be used in large scale processes provided that they last at least for two years in operation.

Another important point extractable from this figure is that normally as the flow rate increases all subcategories of costs increase this is observable in almost all subsections of Fig. 14 except for Fig. 14a at the two lowest flow rates. As can be seen, the lowest TC value is related to F=1000 m^3(STP)/h at membrane lifetime below 6 months, however, after 6 months, the lowest TC value is related to F=1200 m^3(STP)/h. This means that for the membranes with a lifetime over 6 months, which involves the most industrially active membranes, the feed flow rate of 1200 m^3(STP)/h is the most economically interesting number for feed flow rate or the optimum feed flow rate.

We also investigated the effect of the lifetime of the whole system on TC at different membrane areas in each stage. The results are presented in Fig. 15a and b.

As can be seen in this Fig. 15a, TC increases with an increase in membrane area in stage one with a relatively mild slope. However, the increase in TC with the decrease in system lifetime is enormous compared with that with the increase in membrane area. This means that the whole plant lifetime is more critical than the number of modules or membrane surface area in the determination of the economic viability of the system. Moreover, two subfigures of Fig. 14 are compared with each other, it is observed that an opposite trend of TC change exists. This outcome is related to the trade-off between the cost of the turbine and the combined costs of membranes, heat exchangers, and compressors. At fixed feed flow rate, the increase in membrane surface area in stage one causes higher permeate and lower retentate flowrates, hence the combined costs of membranes, heat exchangers, and compressors dominate the costs of a turbine, hence we observe increased TC with membrane surface area. In the case of an increase in membrane surface area in stage 2 (Fig. 15b), the complete opposite scenario happens compared with the first stage surface increase. The reason is that the increased surface area in the second stage does not have an effect as significant as what was observed for the first stage on the cost of the turbine because the retentate flow rate of the second stage is a small percentage of the whole retentate stream entering the turbine hence its effect on turbine costs is not large. However, this small reduction in the cost of the turbine is more effective than the increased combined costs of membranes, heat exchangers, and compressors on TC leading to the observation of TC reduction with an increment in the surface area of membranes in the second stage.

5. Conclusion

In this study which is a combination of experimental work on gas separation membranes and techno-economical analysis of a membrane system configuration, three main aspects were investigated. 1- the utilization of the two most frequently produced food wastes in Iran, for the synthesis of AC powder to be used as particles in the matrix of PVA for CO_2 capture. 2- the sensitivity analysis of a double-stage membrane separation configuration using data from the experimental part of the study to determine the dependency of separation performance criteria such as recoveries, purities, and IGP factor on the main parameters of the system such as module number, feed flowrate and type of membrane and 3- The economic analysis of the system by series of sensitivity analysis to determine the effect of some parameters of the system (membrane lifetime, plant lifetime, membrane area, feed flowrate, and membrane area in each stage) on capital costs, operating costs and total costs of the system.

The experimental part of the work involved membrane synthesis and characterizations with SEM, FTIR, N_2 adsorption-desorption, DFT PSD analysis, and gas permeation tests. The overall result of the experimental part of the work demonstrates that the samples synthesized with AC fabricated by tea wastes showed higher adsorption capacity, BET surface area, CO_2 permeance, and CO_2/CH_4 selectivity compared with their counterparts fabricated from coke wastes. Moreover, the results indicated that with the rise in concentrations of ACs in the matrix of PVA regardless of the type of AC particles, the permeances for both gases increased while the CO_2/CH_4 selectivity decreased. However, all the mixed matrix membranes showed superior separation performance compared with pure PVA membranes.

The results of the technical evaluation part of the work showed that among the four parameters determining the IGP factor, the CO_2 recovery of the system for all membranes was the most influential because it showed the most fluctuations from one membrane to another compared with other factors. The IGP factor was determined to be the maximum for (Tea-AC/PVA-1) sample. The economic evaluation of the system was performed assuming that it was equipped with a (Tea-AC/PVA-1) sample in modules of both stages. The results of this part of the work demonstrate that the costs of the turbine rise exponentially with an increase in flow rate. This outcome with the result of the modeling of work produced by the turbine suggests that the utilization of turbines for generating power is only economically attractive at low flow rates. Moreover, it was observed from the economic analysis that membrane lifetime is a crucial factor in determining the total costs of the system and an economically interesting system should utilize a membrane with at least 6 months of an average lifetime. The whole system lifetime is also critical in total cost calculation and a plant lifetime below 20 years is considered to cause a huge rise in total cost which might lead to economical failure of the proposed membrane system configuration.

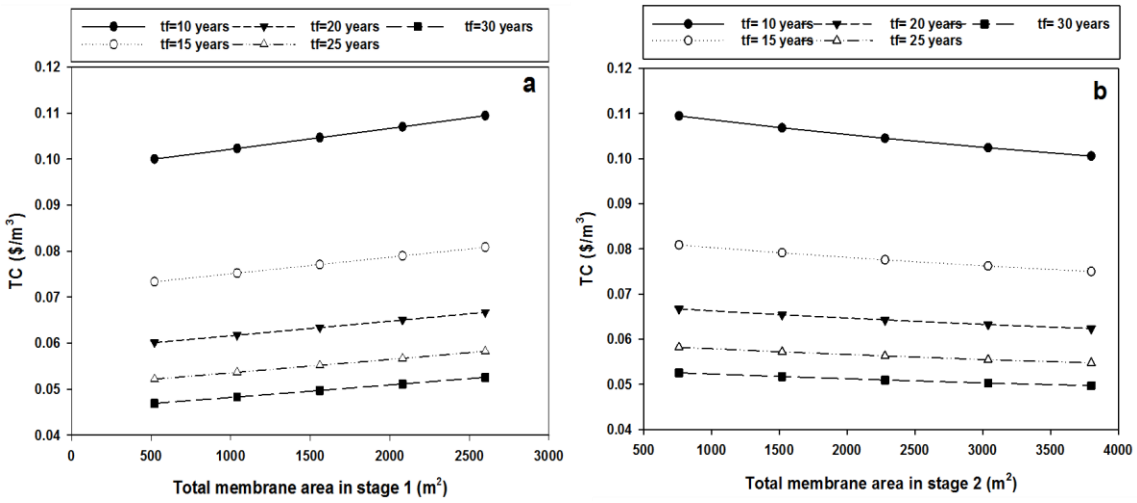

Fig. 15. a) TC versus membrane area at different plat lifetime for a) stage one and b) stage two

CRedit authorship contribution statement

A. Jomekian: Investigation; Methodology; Writing - original draft; Funding; Project administration; Resources.
B. Bazooyar: Software; Validation; Visualization; Writing - review, editing
S.A.A. Mansoori: Data curation; Formal analysis.

Funding

This research did not utilize any source of grants, except for the Esfarayen University of Technology faculty grant.

Declaration of Competing Interest

The authors declare that they have no known competing financial interests or personal relationships that could have appeared to influence the work reported in this paper.

Acknowledgments

The authors express their gratitude to the gas research center of Petroleum University of Technolgy and central lab of Esfarayen University of Technology for providing some facilities for the expriments of this project.

Nomenclature

A_{mem}	total membrane area (m^2)	Q_{FC}	heat exchanged in the first heat exchanger (kW)
AHEFC	total area of heat exchangers (m^2)	Q_{RC}	heat exchanged in the second heat exchanger (kW)
AHERC	area of heat exchanger 1 (m^2)	R	gas constant (kJ/kmol.K)
BPC	area of heat exchanger 2 (m^2)	r_{PFC}	Press. ratio of 1st compressor
C_{ELEC}	cost of electricity ($/y)	r_{PRC}	Press. ratio of 2nd compressor
C_{LS}	loss of energy cost ($/kJ)	$Recovery_{PCO2}$	Recovery of CO_2 at end (%)
C_{pfeed}	heat capacity of the first stage feed (kJ/kmol.K)	$Recovery_{PCH4}$	Recovery of CH_4 at end (%)
C_{prfeed}	heat capacity of the second stage feed (kJ/kmol.K)	SC	costs of start-up ($)
C_{REF}	cost of refrigeration ($/y)	t_f	plant lifetime (y)
CC	capital costs ($/y)	t_{mem}	membrane lifetime (y)
COC	costs of compressors ($/y)	t_{start}	start-up time (y)
COC_{FC}	costs of compressor of the first stage ($/y)	T_{coldFC}	temperature of the entering feed to heat exchanger 1 (°C)
COC_{RC}	costs of compressor of the second stage ($/y)	T_{coldRC}	temperature of the entering feed to heat exchanger 2 (°C)
DLC	direct labor costs ($/y)	T_{hotFC}	elevated temperature of heat exchanger 1 (°C)
F_{in}	flowrate entering the process (m^3 STP/h)	T_{hotRC}	elevated temperature of heat exchanger 2 (°C)
F_{in2}	flowrate entering the second stage (m^3 STP/h)	T_{inREF}	elevated temperature of the second stage heat exchanger (°C)
F_{out}	flowrate exiting the process (m^3 STP/h)	T_{inT}	temperature of inlet stream to turbine (°C)
FC	fixed costs ($)	T_{outREF}	the cooling water temperature at end (°C)
FI	Facilities Investment ($)	TC	total costs ($/$m^3$)
H_v	Lost methane heating value (kJ/m^3)	TUC	costs of turbine ($)
HEC	cost of heat exchangers ($)	U	overall heat transfer coefficient (kW/m^2.K)
IGP	global performance index	UC	utility costs ($/y)
IC	costs of tax and insurance ($/y)	$\dot{V}_{out}$	total permeate flowrate of the process (m^3 STP/h)
ILC	indirect costs of labor ($/y)	$\dot{V}_{out1}$	permeate flowrate of the first stage (m^3 STP/h)
LC	labor costs in total ($/y)	$\dot{V}_{out2}$	permeate flowrate of the second stage (m^3 STP/h)
LSC	loss costs ($/y)	$\dot{V}_D$	daily flowrate of gas entering the system (m^3/d)
MC	maintenance costs ($/y)	$\dot{V}_{LS}$	Lost methane flowrate (m^3/y)
MEC	membrane module costs ($/y)	$\dot{V}_{Treat}$	yearly treated gas flowrate (m^3/y)
MRC	costs of substitution of membrane ($/y)	W_{FC}	work consumed by the first compressor (kW)
n_{LAB}	laborers number	W_{RC}	work consumed by the second compressor (kW)
$\dot{n}_{feed}$	flowrate of gas compressed in stage 1 (kmol/s)	W_T	work generated by the turbine (kW)
$\dot{n}_{Rfeed}$	flowrate of gas compressed in stage 2 (kmol/s)	Z_{ELEC}	price of electricity ($/kW)
$\dot{n}_{Tfeed}$	flowrate of gas entering the turbine (kmol/s)	Z_{LAB}	wage of labor ($/h)
OC	operating costs ($/y)	Z_{mem}	price of membrane ($/$m^2$)
OSF	on-stream factor	Z_{REF}	price of cooling water ($/kJ)
P_{atm}	atmospheric pressure (atm)	α	membrane selectivity
P_{inT}	pressure of turbine feed (atm)	θ_{1FC}	ΔT_1 in heat exchanger 1 (°C)
P_{outFC}	feed pressure entering of the modules of stage 1 (atm)	θ_{1RC}	ΔT_1 in heat exchanger 2 (°C)
P_{outRC}	feed pressure entering of the modules of stage 2 (atm)	θ_{2FC}	ΔT_2 in heat exchanger 1 (°C)
PC	cost of contingencies of project ($)	θ_{2RC}	ΔT_2 in heat exchanger 2 (°C)
Perm	permenace of samples (GPU)	ΔT_{FC}	LMTD of heat exchanger 1 (°C)
PI	project investment ($)	ΔT_{RC}	LMTD of heat exchanger 2 (°C)
$Purity_{PCO2}$	purity of CO_2 at end (%)	η	isentropic efficiency
$Purity_{PCH4}$	purity of CH_4 at end (%)	γ	ratio of C_P/C_V

References

[1] H.S. Fami, L.H. Aramyan, S.J. Sijtsema, A. Alambaigi, Determinants of household food waste behavior in Tehran city: A structural model, Resour. Conserv. Recycl. 143 (2019) 154-166. https://doi.org/10.1016/j.resconrec.2018.12.033.

[2] V. Filimonau, A. Delysia, Food waste management in hospitality operations: A critical review, Tour. Manag. 71 (2019) 234-245. https://doi.org/10.1016/j.tourman.2018.10.009.

[3] A. Sadati, Food waste in Iran; time to return to Islamic perspective of frugality, J. Nutr. Fast. Health 6(4) (2018) 220-221. https://dx.doi.org/10.22038/jnfh.2019.38397.1175.
[4] H.S. Fami, L.H. Aramyan, S.J. Sijtsema, A. Alambaigi, The relationship between household food waste and food security in Tehran city: The role of urban women in household management, Ind. Mark. Manag. 97 (2021) 71-83. https://doi.org/10.1016/j.indmarman.2021.06.016.
[5] M. Najaf Najafi, M. Salehi, M. Ghazanfarpour, Z.S. Hoseini, M. Khadem-Rezaiyan, The association between green tea consumption and breast cancer risk: A systematic review and meta-analysis, Phytother. Res. 32(10) (2018) 1855-1864. https://doi.org/10.1002/ptr.6124.
[6] A. Nabavi-Pelesaraei, R. Bayat, H. Hosseinzadeh-Bandbafha, H. Afrasyabi, K.-w. Chau, Modeling of energy consumption and environmental life cycle assessment for incineration and landfill systems of municipal solid waste management-A case study in Tehran Metropolis of Iran, J. Cleaner Prod. 148 (2017) 427-440. https://doi.org/10.1016/j.jclepro.2017.01.172.
[7] M. Rasapoor, M. Adl, B. Pourazizi, Comparative evaluation of aeration methods for municipal solid waste composting from the perspective of resource management: A practical case study in Tehran, Iran, J. Environ. Manage. 184 (2016) 528-534. https://doi.org/10.1016/j.jenvman.2016.10.029.
[8] S.M.S. Ardebili, Green electricity generation potential from biogas produced by anaerobic digestion of farm animal waste and agriculture residues in Iran, Renewable Energy (2020). https://doi.org/10.1016/j.renene.2020.02.102.
[9] A. Taghizadeh-Alisaraei, S.H. Hosseini, B. Ghobadian, A. Motevali, Biofuel production from citrus wastes: A feasibility study in Iran, Renewable Sustainable Energy Rev. 69 (2017) 1100-1112. https://doi.org/10.1016/j.rser.2016.09.102.
[10] W. Gao, M.R. Farahani, M.K. Jamil, M.K. Siddiqui, H.M.A. Siddiqui, M. Imran, R. Rezaee-Manesh, Kinetic modeling of pyrolysis of three Iranian waste oils in a micro-fluidized bed, Pet. Sci. Technol. 35(2) (2017) 183-189. https://doi.org/10.1080/10916466.2016.1238937.
[11] S. Elkhalifa, T. Al-Ansari, H.R. Mackey, G. McKay, Food waste to biochars through pyrolysis: A review, Resour. Conserv. Recycl. 144 (2019) 310-320. https://doi.org/10.1016/j.resconrec.2019.01.024.
[12] A. Jain, R. Balasubramanian, M. Srinivasan, Hydrothermal conversion of biomass waste to activated carbon with high porosity: A review, Chem. Eng. J. 283 (2016) 789-805. https://doi.org/10.1016/j.cej.2015.08.014.
[13] J.M. Dias, M.C. Alvim-Ferraz, M.F. Almeida, J. Rivera-Utrilla, M. Sánchez-Polo, Waste materials for activated carbon preparation and its use in aqueous-phase treatment: a review, J. Environ. Manage. 85(4) (2007) 833-846. https://doi.org/10.1016/j.jenvman.2007.07.031.
[14] X. Zhang, B. Gao, A.E. Creamer, C. Cao, Y. Li, Adsorption of VOCs onto engineered carbon materials: A review, J. Hazard. Mater. 338 (2017) 102-123. https://doi.org/10.1016/j.jhazmat.2017.05.013.
[15] S.A.A. Mansoori, Z. Reza, H. Mohammad, M.S. Mohammad, J. Abolfazl, S. Sadegh, E. Akbar, HSS anions reduction combined with the analytical test of aqueous MDEA in South Pars gas complex, Nat. Gas Ind. B 9(3) (2022) 318-324. https://doi.org/10.1016/j.ngib.2022.06.004.
[16] W. Fam, J. Mansouri, H. Li, V. Chen, Improving CO2 separation performance of thin film composite hollow fiber with Pebax® 1657/ionic liquid gel membranes, J. Membr. Sci. 537 (2017) 54-68. https://doi.org/10.1016/j.memsci.2017.05.011.
[17] J. Kim, Q. Fu, K. Xie, J.M. Scofield, S.E. Kentish, G.G. Qiao, CO2 separation using surface-functionalized SiO2 nanoparticles incorporated ultra-thin film composite mixed matrix membranes for post-combustion carbon capture, J. Membr. Sci. 515 (2016) 54-62. https://doi.org/10.1016/j.memsci.2016.05.029.
[18] L. Deng, T.-J. Kim, M.-B. Hägg, Facilitated transport of CO2 in novel PVAm/PVA blend membrane, J. Membr. Sci. 340(1-2) (2009) 154-163. https://doi.org/10.1016/j.memsci.2009.05.019.
[19] M. Barooah, B. Mandal, Synthesis, characterization and CO2 separation performance of novel PVA/PG/ZIF-8 mixed matrix membrane, J. Membr. Sci. 572 (2019) 198-209. https://doi.org/10.1016/j.memsci.2018.11.001.
[20] J.Ø. Torstensen, R.M.L. Helberg, L. Deng, Ø.W. Gregersen, K. Syverud, PVA/nanocellulose nanocomposite membranes for CO2 separation from flue gas, Int. J. Greenhouse Gas Control 81 (2019) 93-102. https://doi.org/10.1016/j.ijggc.2018.10.007.
[21] Z. Jahan, M.B.K. Niazi, M.-B. Hägg, Ø.W. Gregersen, Cellulose nanocrystal/PVA nanocomposite membranes for CO2/CH4 separation at high pressure, J. Membr. Sci. 554 (2018) 275-281. https://doi.org/10.1016/j.memsci.2018.02.061.
[22] G. Guerrero, M.-B. Hägg, G. Kignelman, C. Simon, T. Peters, N. Rival, C. Denonville, Investigation of amino and amidino functionalized Polyhedral Oligomeric SilSesquioxanes (POSS®) nanoparticles in PVA-based hybrid membranes for CO2/N2 separation, J. Membr. Sci. 544 (2017) 161-173. https://doi.org/10.1016/j.memsci.2017.09.014.
[23] M. Czyperek, P. Zapp, H. Bouwmeester, M. Modigell, K.-V. Peinemann, I. Voigt, W. Meulenberg, L. Singheiser, D. Stöver, MEM-BRAIN gas separation membranes for zero-emission fossil power plants, Energy Procedia 1(1) (2009) 303-310. https://doi.org/10.1016/j.egypro.2009.01.042.
[24] M. Czyperek, P. Zapp, H.J. Bouwmeester, M. Modigell, K. Ebert, I. Voigt, W. Meulenberg, L. Singheiser, D. Stöver, Gas separation membranes for zero-emission fossil power plants: MEM-BRAIN, J. Membr. Sci. 359(1-2) (2010) 149-159. https://doi.org/10.1016/j.memsci.2010.04.012.
[25] D.E. Koutsonikolas, S.P. Kaldis, G.T. Pantoleontos, V.T. Zaspalis, G.P. Sakellaropoulos, Techno-economic assessment of polymeric, ceramic and metallic membranes integration in an advanced IGCC process for H2 production and CO2 capture, Chem. Eng. Trans. 35 (2013) 715-720. https://doi.org/10.3303/CET1335119.
[26] S. Sharifiana, N. Asasian-Kolura, M. Harasekb, Process simulation of syngas purification by gas permeation application, Chem. Eng. Trans. 76 (2019). https://doi.org/10.3303/CET1976139.
[27] R. Bounaceur, E. Berger, M. Pfister, A.A.R. Santos, E. Favre, Rigorous variable permeability modelling and process simulation for the design of polymeric membrane gas separation units: MEMSIC simulation tool, J. Membr. Sci. 523 (2017) 77-91. https://doi.org/10.1016/j.memsci.2016.09.011.
[28] Á.A. Ramírez-Santos, M. Bozorg, B. Addis, V. Piccialli, C. Castel, E. Favre, Optimization of multistage membrane gas separation processes. Example of application to CO2 capture from blast furnace gas, J. Membr. Sci. 566 (2018) 346-366. https://doi.org/10.1016/j.memsci.2018.08.024.
[29] S. Fujikawa, R. Selyanchyn, T. Kunitake, A new strategy for membrane-based direct air capture, Polymer J. 53(1) (2021) 111-119. https://doi.org/10.1038/s41428-020-00429-z.
[30] J.A. Lie, T. Vassbotn, M.-B. Hägg, D. Grainger, T.-J. Kim, T. Mejdell, Optimization of a membrane process for CO2 capture in the steelmaking industry, Int. J. Greenhouse Gas Control 1(3) (2007) 309-317. https://doi.org/10.1016/s1750-5836(07)00069-2.
[31] X. He, J.A. Lie, E. Sheridan, M.-B. Hägg, CO2 capture by hollow fibre carbon membranes: Experiments and process simulations, Energy Procedia 1(1) (2009) 261-268. https://doi.org/10.1016/j.egypro.2009.01.037.
[32] X. He, M.-B. Hägg, Hollow fiber carbon membranes: Investigations for CO2 capture, J. Membr. Sci. 378(1-2) (2011) 1-9. https://doi.org/10.1016/j.memsci.2010.10.070.
[33] F. Ahmad, K.K. Lau, A.M. Shariff, G. Murshid, Process simulation and optimal design of membrane separation system for CO2 capture from natural gas, Comput. Chem. Eng. 36 (2012) 119-128. https://doi.org/10.1016/j.compchemeng.2011.08.002.
[34] D. Grainger, M.-B. Hägg, Techno-economic evaluation of a PVAm CO2-selective membrane in an IGCC power plant with CO2 capture, Fuel 87(1) (2008) 14-24. https://doi.org/10.1016/j.fuel.2007.03.042.
[35] J. Huang, J. Zou, W.W. Ho, Carbon dioxide capture using a CO2-selective facilitated transport membrane, Ind. Eng. Chem. Res. 47(4) (2008) 1261-1267. https://doi.org/10.1021/ie070794r.
[36] R. Khalilpour, A. Abbas, Z. Lai, I. Pinnau, Modeling and parametric analysis of hollow fiber membrane system for carbon capture from multicomponent flue gas, AIChE J. 58(5) (2012) 1550-1561. https://doi.org/10.1002/aic.12699.
[37] N.C. Mat, G.G. Lipscomb, Membrane process optimization for carbon capture, Int. J. Greenhouse Gas Control 62 (2017) 1-12. https://doi.org/10.1016/j.ijggc.2017.04.002.
[38] J. Xu, Z. Wang, Z. Qiao, H. Wu, S. Dong, S. Zhao, J. Wang, Post-combustion CO2 capture with membrane process: Practical membrane performance and appropriate pressure, J. Membr. Sci. 581 (2019) 195-213. https://doi.org/10.1016/j.memsci.2019.03.052.
[39] M. Binns, S. Lee, Y.-K. Yeo, J.-H. Lee, J.-H. Moon, J.-G. Yeo, J.-K. Kim, Strategies for simulation of multi-component hollow fiber multi-stage membrane gas separation systems, J. Membr. Sci. 497 (2016) 458-471. https://doi.org/10.1016/j.memsci.2015.08.023.
[40] B. Liu, X. Yang, T. Wang, M. Zhang, P.-C. Chiang, CO2 separation by using a three-stage membrane process, Aerosol Air Qual. Res. 19(12) (2019) 2917-2928. https://doi.org/10.4209/aaqr.2019.10.0519.
[41] L. Giordano, J. Gubis, G. Bierman, F. Kapteijn, Conceptual design of membrane-based pre-combustion CO2 capture process: Role of permeance and selectivity on performance and costs, J. Membr. Sci. 575 (2019) 229-241. https://doi.org/10.1016/j.memsci.2018.12.063.
[42] A. Jomekian, R.M. Behbahani, Experimental, Modeling and AspenPlus Simulation of Different Configurations of Membrane Separation Systems for Highly Loaded CO2 Selective Pebax 1657-ZIF-8 Membrane, J. Membr.

Sci. Res. 7(3) (2021) 209-223. https://doi.org/10.22079/jmsr.2020.136920.1411.
[43] R. Abejón, C. Casado-Coterillo, A. Garea, Techno-Economic Optimization of Multistage Membrane Processes with Innovative Hollow Fiber Modules for the Production of High-Purity CO2 and CH4 from Different Sources, Ind. Eng. Chem. Res. (2022). https://doi.org/10.1021/acs.iecr.2c01138.
[44] M. Smith, H. Van Ness, M. Abbot, Introduction to Chemical Engineers Thermodynamics, Chemical Engineering Series, McGraw-Hill (2005).
[45] A. Aliaga-Vicente, J.A. Caballero, M.J. Fernández-Torres, Synthesis and optimization of membrane cascade for gas separation via mixed-integer nonlinear programming, AIChE J. 63(6) (2017) 1989-2006. https://doi.org/10.1002/aic.15631.
[46] M.S. Peters, K.D. Timmerhaus, R.E. West, Plant design and economics for chemical engineers, McGraw-hill New York2003.
[47] M. Malhotra, S. Suresh, A. Garg, Tea waste derived activated carbon for the adsorption of sodium diclofenac from wastewater: adsorbent characteristics, adsorption isotherms, kinetics, and thermodynamics, Environ. Sci. Pollut. Res. 25(32) (2018) 32210-32220. https://doi.org/10.1007/s11356-018-3148-y.
[48] Y. Ju, Y. Park, D. Park, J.-J. Kim, C.-H. Lee, Adsorption kinetics of CO2, CO, N2 and CH4 on zeolite LiX pellet and activated carbon granule, Adsorption 21(5) (2015) 419-432. https://doi.org/10.1007/s10450-015-9683-7.
[49] L. Deng, M.-B. Hägg, Techno-economic evaluation of biogas upgrading process using CO2 facilitated transport membrane, Int. J. Greenhouse Gas Control 4(4) (2010) 638-646. https://doi.org/10.1016/j.ijggc.2009.12.013.
[50] S. Haider, A. Lindbråthen, M.-B. Hägg, Techno-economical evaluation of membrane-based biogas upgrading system: A comparison between polymeric membrane and carbon membrane technology, Green Energy Environ. 1(3) (2016) 222-234. https://doi.org/10.1016/j.gee.2016.10.003.